GARTEUR GROUP ON GROUND VIBRATION TESTING. RESULTS FROM THE TEST OF A SINGLE STRUCTURE BY 12 LABORATORIES IN EUROPE.

Etienne Balmès
DRET / AC, ONERA, Structures Department
B.P.72, 92322 Chatillon Cedex, FRANCE
Jan Wright
University of Manchester
Manchester, M13 9PL, U.K.

ABSTRACT

In an effort to assess state of the art methodologies for the experimental determination of modal characteristics, 12 European groups, most of them working in the area of aircraft ground vibration tests for flutter certification, participated in a GARTEUR action group whose main activity was to have independent tests of a single representative structure. Design considerations for the common structure are first detailed. Estimates of frequency response functions and modal characteristics are then compared and show a level of consistency that is much higher than those reported in previous similar exercises.

1. INTRODUCTION

In the certification of new aircraft, Ground Vibration Tests (GVT) play an important role for the verification or updating of analytical models, allowing more accurate aeroelastic predictions. Facing the risk of flutter, a high level of quality and reliability in obtaining the modal characteristics of the aircraft has to be achieved during the GVT.
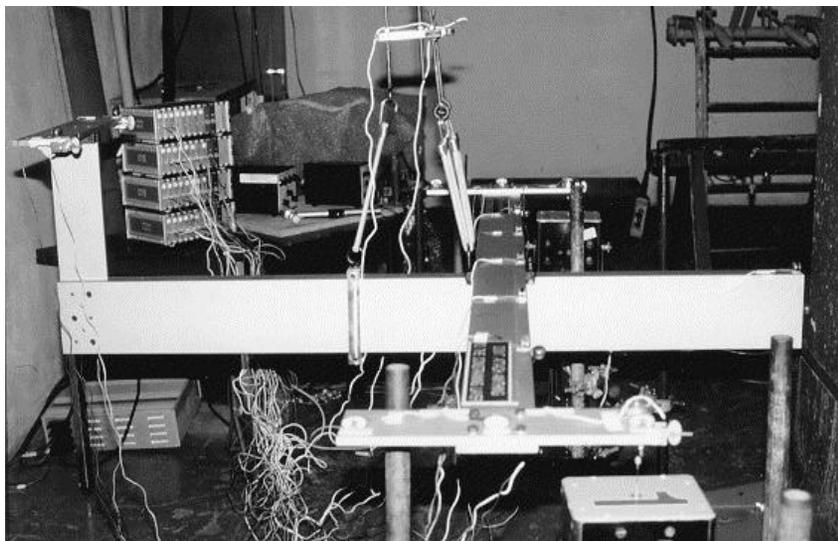
Figure 1: Common testbed of the GARTEUR SM-AG-19.

Following a series of previous Round Robin surveys held in the early 60s [1] and late 70s [2], a Structures and Materials Action Group SM-AG-19 of GARTEUR (Group for Aeronautical Research and Technology in Europe) was initiated in April 1995 with the major objective to compare a number of current

measurement and identification techniques applied to a common structure. The testbed (see figure 1) was designed and manufactured by ONERA (France) and investigated by various companies, research centers and universities from France (ONERA, SOPEMEA, Aérospatiale, Intespace, CNAM), Germany (DLR), the Netherlands (NLR, Fokker), Sweden (Saab) and the United Kingdom (DRA, Manchester University, Imperial College).

More specifically, the objectives of the GVT tests were to evaluate the efficiency and reliability of test methods and to identify the cause of discrepancies between measured frequency responses or identified modal parameters. Each participant was required to provide:

- a set of 4 transfer functions corresponding to excitation and response of the left and right wing tip body (called *drums* in the rest of the paper) in the 4-60 Hz band. Although not required, most participants provided a 2 input 24 output set of transfer functions.

- estimated modal parameters (modeshape, frequency, damping factor, and modal mass) at 24 reference accelerometer locations.

The present paper outlines the activity of SM-AG-19 and compares data provided by the participants. Design considerations for the testbed are discussed in section 2. Frequency response measurements are compared in section 3 and modal parameters in section 4. In the comparisons, participants are identified by letters in chronological testing order. Some data sets obtained in a configuration differing from the test guidelines (see more details in section 2) are not comparable and are thus not included.

2. DESIGN CONSIDERATIONS
Specifications for the testbed were

- a group of 3 very close modes to make the problem difficult.

- 5 to 60 Hz, 50-100 kg, 2 by 2 m to make the testbed suitable for instrumentation designed for aircraft.

- a joint at the wing/fuselage connection for transportation but limiting variability from assembly to assembly.

- damping treatment to limit the effect of dissipation linked to instrumentation.

- suspension by a common set of bungees to have similar boundary conditions.

• 24 common sensor and 2 common shaker locations to allow direct comparisons.

The most difficult design criterion was the presence of 3 very close modes. On such a simple structure, close modal spacing can only be achieved by using modes of a different nature (bending modes in different directions, torsion modes, wing modes vs. tail modes). The relatively massive fuselage induces a near decoupling of torsion modes for each half wing, so that the first two torsion modes come as a pair. The design thus mostly adjusted the drum mass to put the frequency of the 2 torsions close to another mode (the 3 node bending eventually). As shown in figure 2, Nyquist plots of the final testbed show near the resonance a single lobe or three very coupled circles depending on the sensor.
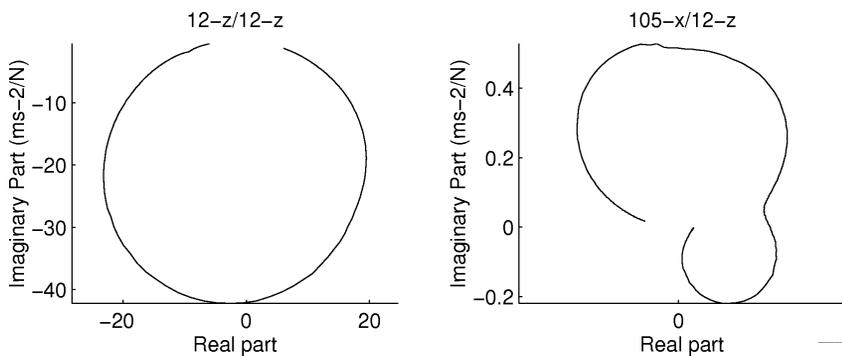
Figure 2: Nyquist plots near the resonance. A single circle is found on some transfer functions while the three modes are always very coupled.

To measure force, participants used load cells or electrical impedance (force/current factor on a current driven shaker). With the second technique, the moving mass, stiffness and damping of the shaker becomes part of the measured structure. On an aircraft the moving masses are so small that the effect is negligible, but for this small testbed a way to compensate for the added mass was needed. The design thus placed a 200g compensation mass at each drum tip (as shown in Fig. 3). In a case where additional mass was known to be added, the nominal mass could thus be replaced by a smaller one to physically compensate for the effect (the fact that the mass position does not exactly coincide with the expected shaker position was not taken into account).
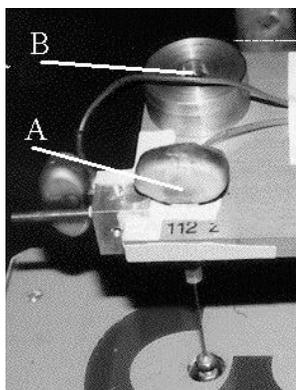
Figure 3: Shaker attachments on the axes of the accelerometer (A) or the compensation mass (B).

The mass sensitivity, of the torsion modes in particular, significantly helped the design but was also one of the major sources of variations in the results of different tests. Inappropriate mass compensation was used for some tests so that not all data sets could be included in the comparisons of sections 3 and 4. Some groups also positioned their shaker on the mass axis rather than on the accelerometer axis (positions A and B in figure 2). The resulting data sets from different groups are clearly different (see following sections).

Sufficient damping levels were obtained through the use of a viscoelastic layer with an aluminum constraining layer. The viscoelastic used is the 3M acrylic viscoelastic polymer ISD 112 in the form of a 76 mm by 50 *mm* roll. A sample roll (Ref: SJ 2015 Type 1202) was provided by 3M Laboratories (Europe), Hansastr. 9, 41453 Neuss, Germany. This viscoelastic is particularly well suited for the testbed operating range of 5-50 Hz and 20 C where the loss factor is near its peak of 0.9.

Significant levels of shear strain are obtained in the viscoelastic through the use of a 1.1 x 76.2 x 170 mm constraining layer covering the complete viscoelastic treatment. The ISD 112 being pressure sensitive, the bonding was obtained easily and 3M confirmed that only extreme conditions should damage it. In a wing only test, damping factors increased significantly (from 0.28% to 1.1% in bending at 9 Hz and from 0.15% to 0.86% in torsion at 27 Hz) with the added treatment. Tests done on different days gave very similar results.
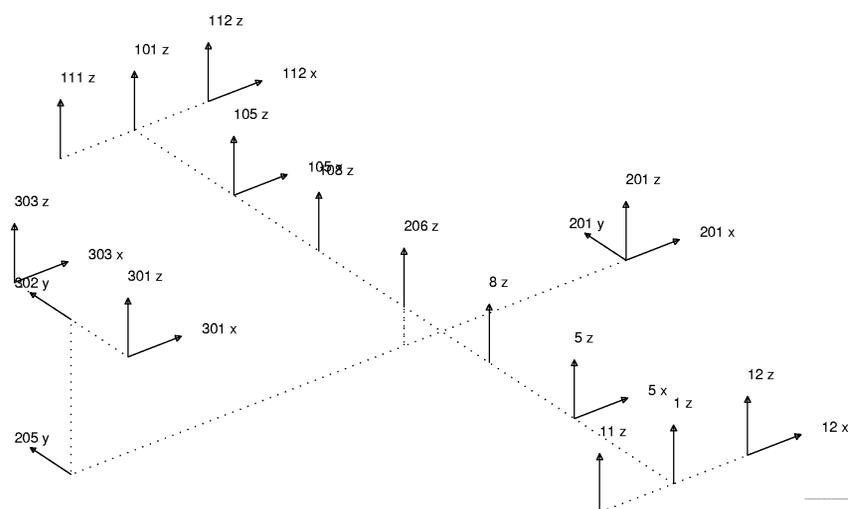
Figure 4: 24 common accelerometer locations. Nominal excitation locations are 12-z and 112-z.

Table 1 : Check of the sensor placement using the MAC comparison of a set of experimental modes with themselves.

Mode	1	2	3	4	5	6	7	8
1	100.0	0.0	0.2	1.6	0.5	18.1	0.0	0.1
2	0.0	100.0	0.5	0.2	0.0	0.1	0.1	0.0
3	0.2	0.5	100.0	0.3	11.8	1.7	0.5	0.1
4	1.6	0.2	0.3	100.0	1.1	1.8	0.1	2.0
5	0.5	0.0	11.8	1.1	100.0	0.8	21.3	0.0
6	18.1	0.1	1.7	1.8	0.8	100.0	0.5	0.4
7	0.0	0.1	0.5	0.1	21.3	0.5	100.0	0.4
8	0.1	0.0	0.1	2.0	0.0	0.4	0.4	100.0

The common 24 sensor locations, shown in figure 4, were chosen by hand early in the design process. As shown in table 1 by the

17/03/97

off-diagonal terms of the Modal Assurance Criterion (MAC [3]) comparison of an experimental mode set with itself, this set of sensors has problems distinguishing mode pairs 1-6, 3-5 and 5-7. The fact that modes 3-5 are very close in frequency is an additional difficulty. No simple weighting of the sensors seems to significantly improve the geometrical independence of these 3 mode pairs.

Figure 5 shows the 9 modeshapes measured by participant C. The second mode was used as a check of proper assembly. As will be shown in section 4, it was effectively the most consistently estimated mode. *A posteriori*, it should be said that this choice was not ideal since this mode was among the least sensitive to perturbations and thus not informative on the fact that the test configuration specification was met.

1 @ 6.376 Hz 1.30 %   2 @ 16.104 Hz 1.30 %   3 @ 33.125 Hz 0.83 %

4 @ 33.531 Hz 1.00 %   5 @ 35.647 Hz 1.10 %   6 @ 48.384 Hz 2.30 %

7 @ 49.433 Hz 0.46 %   8 @ 55.076 Hz 0.20 %   9 @ 63.039 Hz 2.00 %
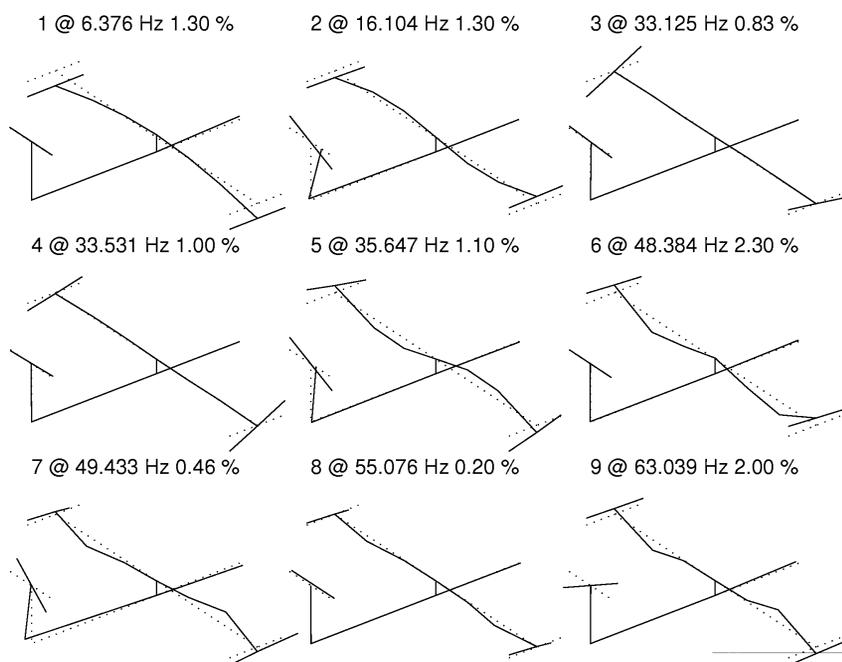
Figure 5. Set of modes measured by participant C.

For all tests, the structure was suspended using bungees linked to a small plate common to all the participants (as shown in figure 1). The participants were however free to attach the plate in any appropriate manner. Some fixed the plate to a hard point while others used pendulums of various lengths. Table 2 shows however no direct relation between pendulum length and estimated rigid body heave mode.

Table 2 : Length of suspension pendulum (length of bungees not included) and estimated frequency of heave mode.

Set	B	C	E-F	G	H	I
Length (m)	12.0	0.0	2.6	0.7	0.4	0.9
Freq (Hz)	1.88	1.8	2.7	2.2	2.6	2.4

3. COMPARISON OF MEASURED FRF

The participants were required to provide a 2 by 2 set of transfer functions with 2 collocated transfers (point mobilities) at the drum tips (12z and 112z) and 2 cross transfers (12z to 112z, 112z to 12z). The collocated transfers are expected to be equal because of the symmetry of the structure, and the cross transfers because of reciprocity.

Figures 6 shows a comparison of the 112z collocated transfers measured by a number of participants. General trends are clearly common to all measurements. Above 40 Hz, the response is however dominated by modes near 34 Hz so that it is hard to see how coherent the measurements are. Tests B and J show significant discrepancy near 35 Hz, these are however easily explained by the selection of inappropriate compensation masses.

The collocated transfers 12z are slightly different from those of figure 6 because the structure is not really symmetric (manufacturing tolerances led to a non symmetric wing), but otherwise show little more information.
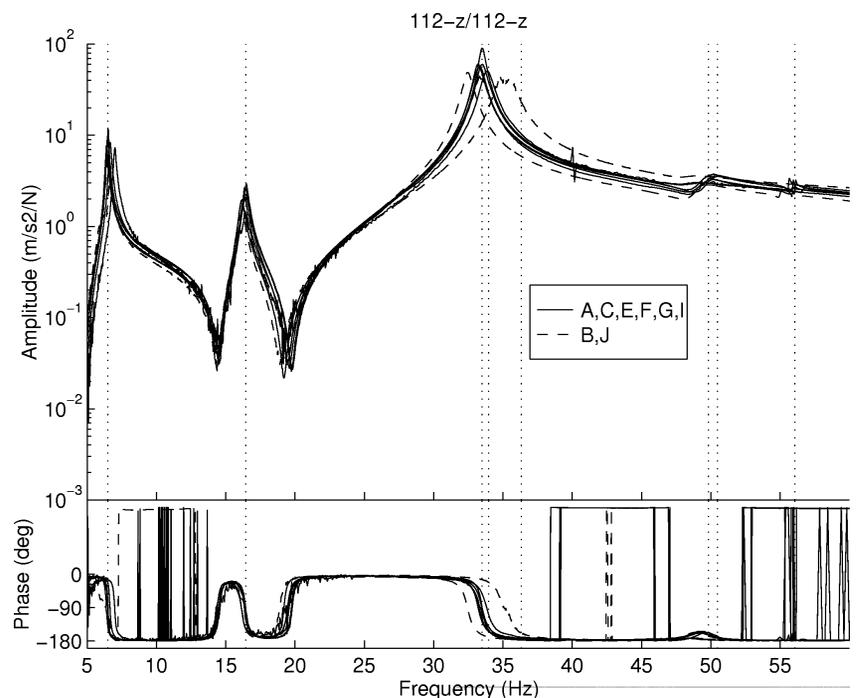
Figure 6. Collocated transfer function at left drum (112z).
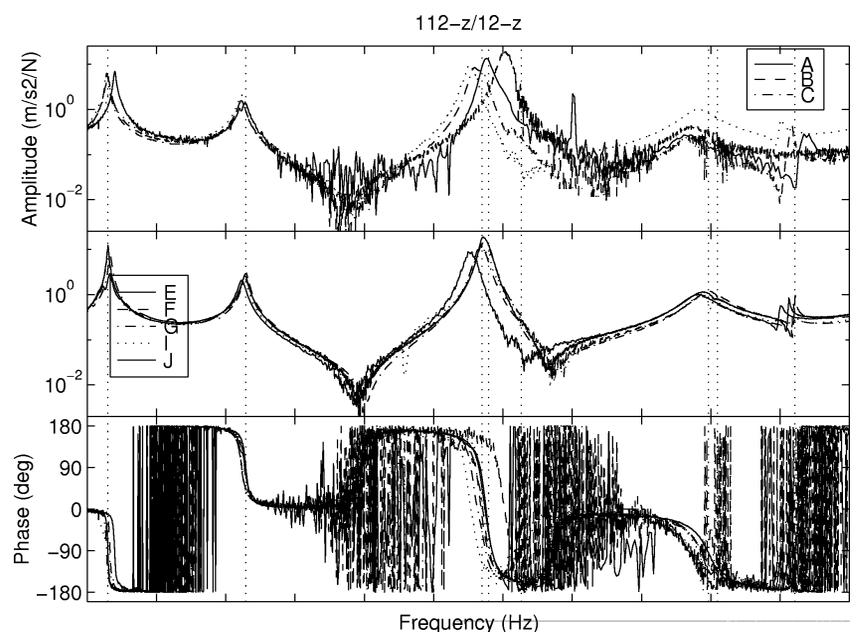
Figure 7. Cross transfer 112z to 12z. Amplitude plots are separated in two groups depending on shaker position (A and B in figure 3).

The required cross transfers (12z to 112z shown in figure 7) are much more informative. Some data sets are very noisy and/or show quantization errors. Data set A has for example a fairly high noise floor, which masks the anti-resonances of cross transfers. It

must be noted however that the groups who provided noisy data sets do not use FRF data for identification purposes.

Resonance frequencies show significant variability from test to test. For example, the resonance of the first mode goes from 6.4 to 7 Hz. These variations are coherent with the modal results given by the participants. Despite frequency shifts, the general trends (positions of resonances and anti-resonances) are well preserved in all data sets. Sets B and J have again the resonances of the torsion modes shifted up and down respectively.

Figure 7 distinguishes sets ABC from sets EFGJ based on where the shaker was attached (positions A and B of figure 4). Above 35 Hz, the two sets show a significant difference in the level of response. Within each set, the responses are however coherent.
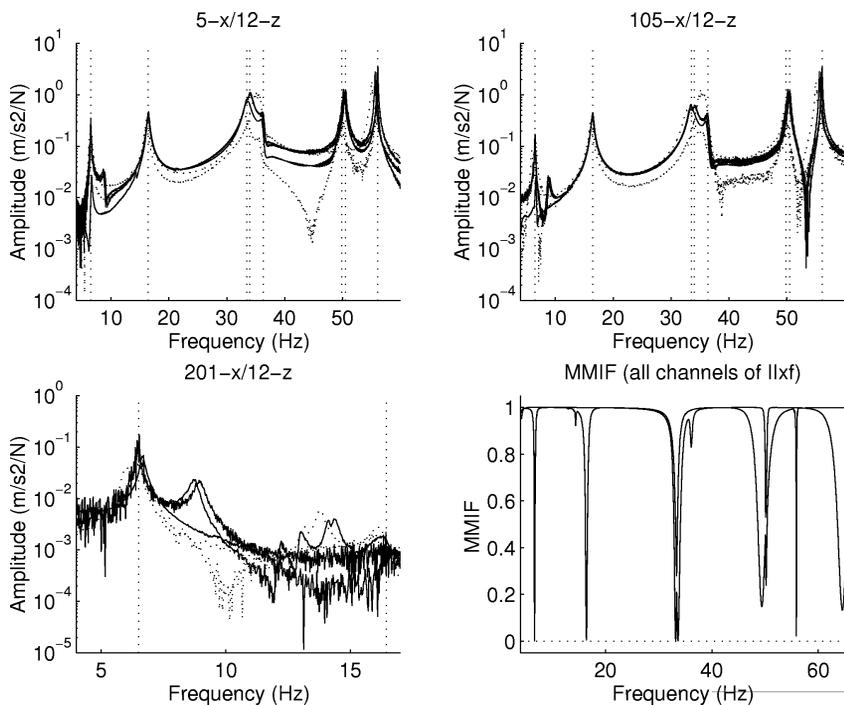
Figure 8. **A-B** cross transfers 12z to 5x and 105x. **C** low frequency range of 201x/12z. **D** Multivariate Mode Indicator Function [4] for inputs 12z and 112z

Figure 8a and 8b show transfers between drum excitation and the in plane mid wing sensor. Sets AC which are very noisy for these sensors have been removed. Sets B,J are shown in dotted lines and one sees the frequency shifts near 35 Hz. Set J significantly differs from other sets which may account for the discrepancies seen for modeshapes (see section 4).

Sensors 5x, 105x and sensor 201x even more (figure 8c) indicate the presence of many suspension modes in the 5-15 Hz range. These modes are hardly seen in the response of vertical sensors except for group J which was unlucky enough to have the frequency of 2 suspension modes coincide with the 2 node bending.

Drops in the second mode indicator function of figure 8d clearly indicate the presence of the two torsions (33.8 Hz) and tail torsion (49.4 Hz). The 3 node bending (35.7 Hz) is however not very well excited (the minimum of the MIF is above 0.8) which shows that these shaker positions are not suited for a force appropriation of this mode.

One should also note that the force measurement technique (groups ACG use current, others use load cells) or the input signal used (participants used stabilized and swept sine, single and multiple input broadband signals) do not appear to have any significant influence. Noise levels seem to be inversely proportional to how much use was made of them for identification purposes. Even for groups using identification, responses to non reference inputs were used to identify some modes (3 bending and in plane modes in particular).

As a check for the variability of results, the test was performed at ONERA in the middle and the end of the testing period. The two tests differ by shaker stinger, shaker suspension, testbed bungees, excitation level. The results shown in figure 9 are thus a case where a marginal evolution of test conditions leads to visible differences in the test response. The change in noise level is related to a change in the algorithm used to detect stabilization in a stepped sine but shifts of resonance frequencies are clearly apparent. It is not possible to tell whether these are due to modifications of the structure or the test set-up but they are significant and of the same order as variations seen between results of different participants. Further tests will be performed to clarify this issue.
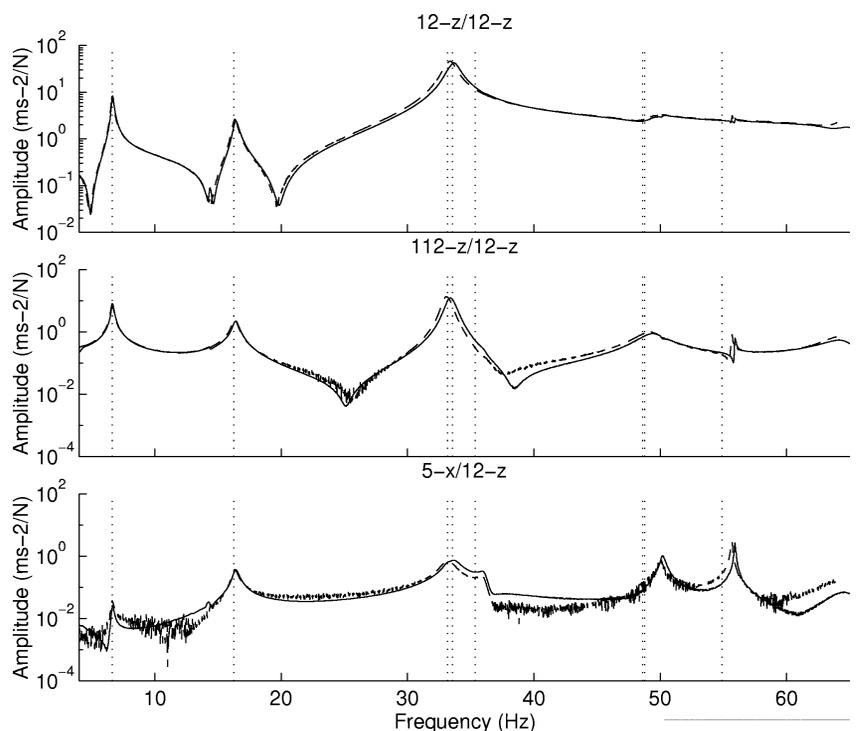
Figure 9. Comparison of two tests performed by ONERA.

4. COMPARISON OF MEASURED MODES

The second part of the exercise was to provide estimates of modal characteristics: frequency, damping ratio, modeshape and modal mass.

Participants ACEGH provided results obtained using force appropriation methods, while other results are based on model identification from measured transfer functions. The results shown do not indicate any influence of the method used on the results obtained.

Figure 10 shows the typical spread of identified modes to be close to 4 %. Many frequency discrepancies can be related to structural modifications linked to the instrumentation or selection of compensation masses. For example, an insufficient compensation mass leads for test B to the high frequency estimate of the 2 torsion modes (33.45 and 33.89 Hz). No simple explanation of the high variability of mode 1 frequencies was however found.

For damping ratios, the typical spread is closer to 30%. Modes 7 and 8 show the highest variations but also have the lowest damping values. This only confirms the fact that very lightly damped modes are difficult to characterize. In particular, instrumentation is likely to contribute most of their damping so that one should not expect their damping values to stay constant. This expected sensitivity was the main reason to design a damping treatment to increase the overall damping of the testbed.
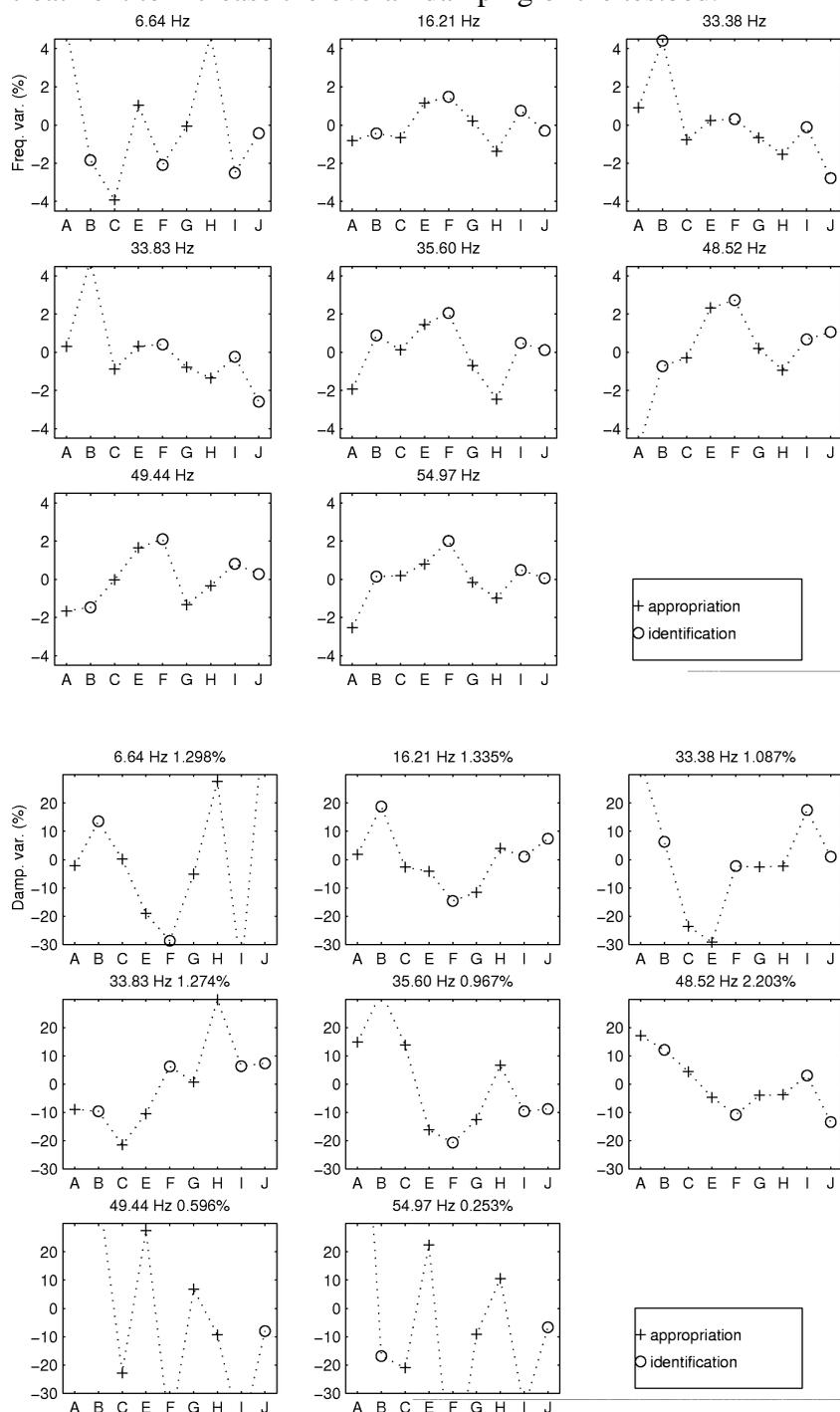
Figure 10. Variations in estimated modal frequencies and damping ratios.

Another question of interest is the sensitivity of the results to the method used. The plots do not indicate any particular trend that would be characteristic of either identification or force appropriation. To confirm that the variability of results is indeed linked to changes in the structure/test setup and not the method, the IDRC [5] identification method was used on available data sets to provide independent estimates of modal frequencies.

For the three close modes, figure 11 shows that the only visible frequency variations from the participants results are found for the 3 node bending for groups ACEG. These groups used force

appropriation and good appropriation of the 3 node bending cannot be achieved with the drum tip shakers only. These groups thus had to use another shaker and, given the modification of the test setup, variations of frequencies are expected. Group C, who attached the shaker to the fuselage, minimized this effect and the frequency difference is low. The FRFs of this group to the 2 reference inputs are not however consistent (resonance frequencies shift when the input is changed). The identification was thus performed on a single excitation which may explain the relatively poor MAC comparison of torsion modeshapes. On real aircraft, dependence on input location is often linked to the presence of non linearities. On the considered testbed it is more likely that the instrument loading changed between tests.
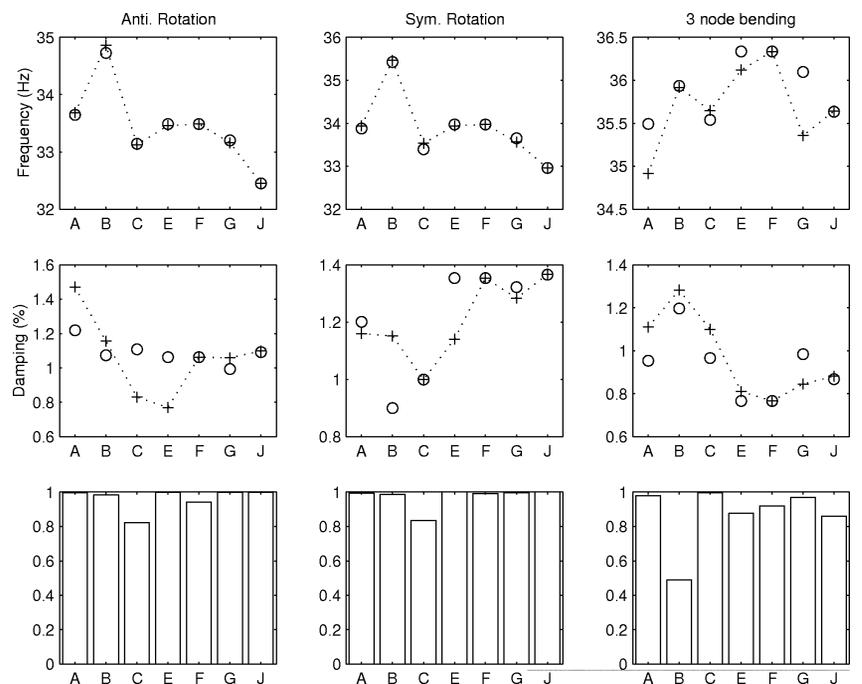
Figure 11. Comparison of the 3 close modes given by the groups with results independently identified from their FRF data (IDRC method).

The participants were all asked to compare their results with those of test A. This test however happens to have rather different modes 4 and 5 so that set C will be used as reference here. The MAC comparisons shown in figure 12 indicate a very good overall correlation. A few poor modes (mode 2 set E, 7 set F, 8 set H) are really exceptional errors of these groups. The only real difficulties are linked to the three closely spaced modes (modes 3-5).
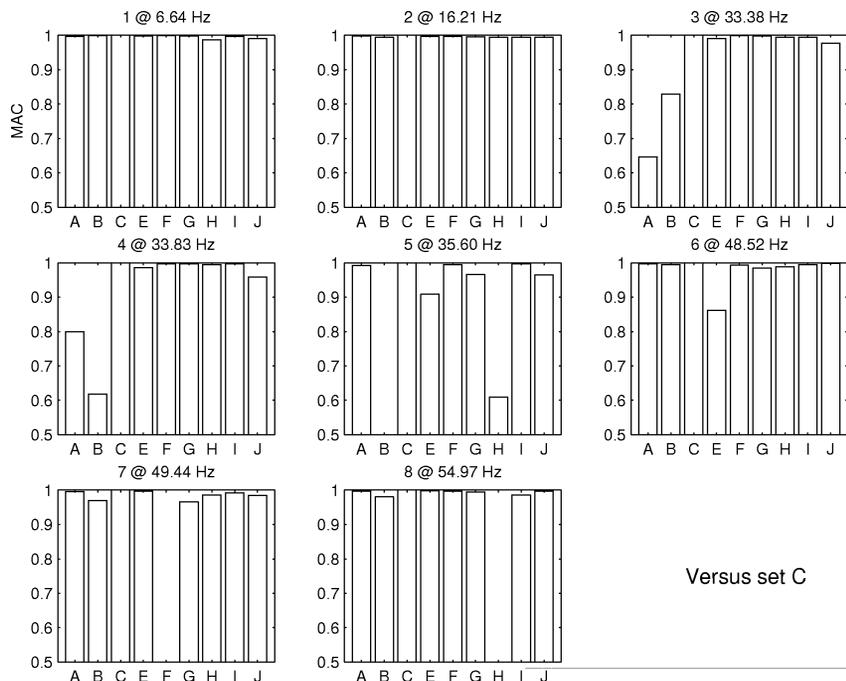
Figure 12. Diagonal MAC values for comparison of different test modeshapes with those of test C.
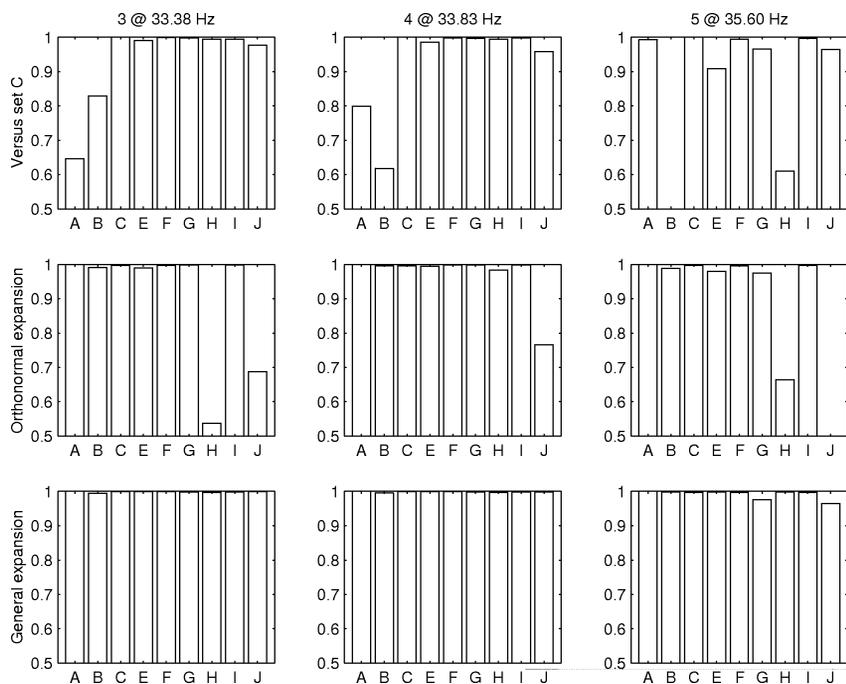
Figure 13. a) MAC comparison with test C
b) Comparison after orthonormal expansion
c) Comparison after general expansion.

It is well known that modes that are close in frequency can be very sensitive to small modifications of the structure. The symmetric and antisymmetric torsions (modes 3-4) and the 3 node bending (mode 5) are very sensitive to mass stiffness modifications. Since the instrumentation of each participant is expected to vary, non-negligible perturbations are expected. Such perturbations however will only induce recombination of modes that are close in frequency (this is the case of modes 3-5). It could be further argued that the recombination should be almost orthogonal since orthogonality conditions always exist even for modes with equal frequencies.

A general linear combination and an orthogonal linear combination of the basis of the modeshapes 3-5 is done to improve the match between each set and set C. The resulting comparison of modeshapes (shown in Fig. 13) shows a very

significant improvement over the results of Fig. 12. Even for the orthonormal expansion, only sets H and J have difficulties which may be explained by a poor orthogonality and/or normalization of the results given by these groups.

Modal masses are the last step of the comparison. Rather than comparing modal masses which would be sensitive to the choice of a particular scaling sensor, it is preferred here to consider mass normalized modeshapes such that the reconstructed FRF are given by

$$H_{kl} = \sum_{j=1}^{N} \frac{(c_k f_j)(f_j^T b_l)}{s^2 + 2z_j w_j s + w_j^2} \quad (1)$$

where c_k and b_l are used here to represent the extraction of the proper component of the measured modeshape. When the scaled modeshapes are known at the 24 sensors, the scaling error can be measured using the scaling coefficient f

$$f_{AB} = \frac{(c_k f_j)_{Test A}^T (c_k f_j)_{Test B}}{(c_k f_j)_{Test A}^T (c_k f_j)_{Test A}} - 1 \quad (2)$$

which should be close to 0. Table 3 shows the values of coefficient f_{AB} for a comparison with the 8 modes of set C. The scaling coefficient is only appropriate if the modeshapes are similar, so that scaling coefficients corresponding to low MAC values are shaded in the table and should not be considered for the comparison. The table clearly indicates that typical mass normalization errors are below 10%.

Table 3 : scale factor (2) and variation in estimated damping (in %) for a comparison of mass normalized modes given by different groups. Shaded elements correspond to low MAC (see Fig. 12).

Mode	A		C		E		F		G	
In %	f	Dz	f	Dz	f	Dz	f	Dz	f	Dz
1	-3	-2	0	0	9	-19	3	-29	3	-5
2	-7	5	0	0	5	-2	8	-12	-4	-9
3	-21	77	0	0	5	-7	6	28	0	28
4	-17	16	0	0	0	14	7	35	6	28
5	7	1	0	0	2	-26	12	-30	3	-23
6	-6	12	0	0	-8	-9	20	-15	-3	-8
7	-6	98	0	0	10	65	-96	-28	-6	38
8	-4	180	0	0	-17	55	7	-56	-1	15

Most identification methods tend to preserve the response at resonance ($s = iw_j$). From (1), an error on the damping ratio z_j would thus tend to be compensated by an error in the same direction on the modal mass. The damping variations shows in the table are clearly much more significant than the modal mass variations so that the variations cannot be attributed to bad identification. It seems that damping changed from test to test, while modal mass was properly identified and is, as expected, independent of the damping level.

6

Figure 14 shows for groups CEG, the absolute value of the mass normalized modeshapes $c_k t_j$ at the 24 sensors. The overall comparison is very good. One can note the dissymetry of the torsion modes 3 and 4 (the pairs of high peaks correspond to right and left vertical sensors at drum tips). For modes 5 and 6, the low MAC (below 0.9) shown in figure 12 now appears as variations in the wing (mode 5) and tail (mode 6) motion.

One can again try to see if the results found depend on the parameter extraction method used. For mode 2, the IDRC identification algorithm was again used on data sets EFGJ. The resulting mass normalized modeshape is shown in figure 15 where only very minor variations are seen (the error on sensor 20 group E is just a calibration problem). For sets ABC, the results are also very similar but an identical scale difference is found which is easily explained by the fact that these groups excited at point B (see figure 3).
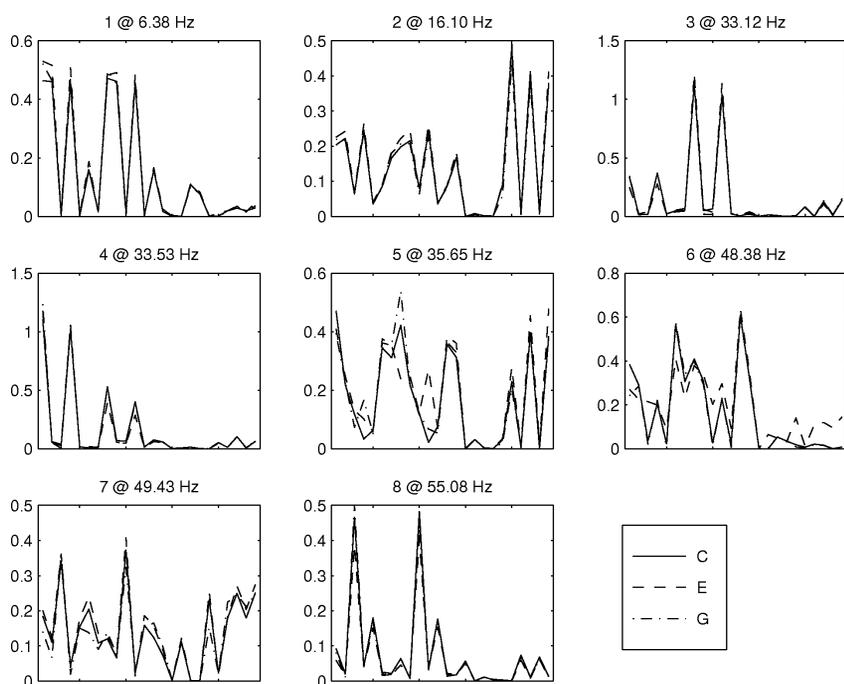
Figure 14. Mass normalized modeshapes given by participants at the 24 sensors.
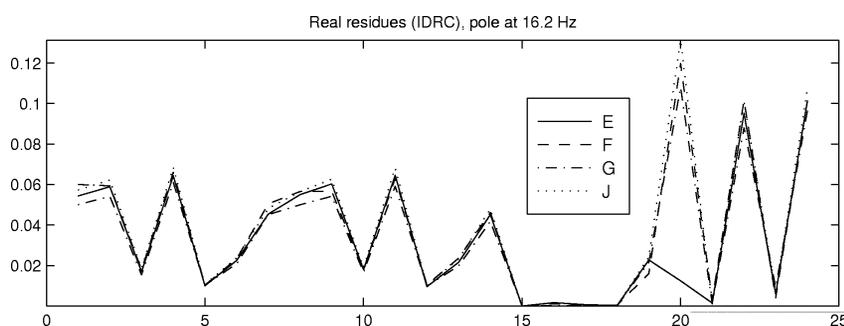
Figure 15. Mass normalized shape of mode 2 found by IDRC identification using different data sets.

5. CONCLUSIONS

Although the methods and hardware used by different participants were widely different, the results compare very well. Force measurement techniques through load cell or current measurements did not lead to any visible modification of the frequency responses.

Force appropriation and identification methods led to very similar modeshape estimates. Identification results were however generally given as complex modes. Simple methods were used to determine normal modes but vector normalization was often lost in this process. Variability in frequencies were of the order of 4%, in damping of the order of 30%. Variability in estimated modal masses were, for the groups who provided mass normalized normal modes, below 10% which leads to think that damping truly varied significantly from test to test while participants were able to properly identify mass normalized modeshapes.

The force appropriation of certain modes implies the use of additional shakers which, for this small testbed, introduces modifications linked to instrument loading. The testbed is mostly linear, has only one difficulty with closely spaced modes and uses a small number of sensors. None of the main reasons that make force appropriation useful are met. The results still compare extremely well.

Many of the important variations between the various test results could be traced back to inappropriate mass compensation of the shaker moving mass, or mass and stiffness loading of the structure by instruments or suspension. For tests performed a year apart by the same team, visible variations were found without having the possibility to determine if these were due to changes in the structure or the test conditions. This highlights the difficulty of obtaining the desired test conditions or simply characterizing the effect of the actual instrumentation.

Future group activities will be to compare identification results on a common data set, in an exercise similar to the SVIB Round Robin [6] but based on actual test data, and to analyze strategies considered for shaker and sensor placement.

6. REFERENCES

[1] Remmers, G.M., Belsheim, R.O. "Effects of technique on reliability of mechanical impedance measurement," *Shock and Vibration Bulletin,* **34**-3, 1964

[2] Ewins, D.J., Griffin, J., "A State of the Art Assessment of Mobility Measurement Techniques – Results for the Mid-Range Structures (30-3000 Hz)," *Journal of Sound and Vibration*, 1981, **78**-2, p. 197-222

[3] Avitabile, P., O'Callahan, J., Milani, J., "Model Correlation and Orthogonality Criteria," *IMAC*, 1988, pp. 1039-1047

[4] Williams, R., Crowley, J., Vold, H., "The Multivariate Mode Indicator Function in Modal Analysis," *IMAC*, 1985, p. 66-70

[5] Balmès, E., "Frequency domain identification of structural dynamics using the pole/residue parametrization," *IMAC*, 1996, p. 540-546

[6] Ahlin, K., "Round Robin Exercise on Modal Parameter Extraction," *IMAC*, 1996, pp.